*Int. J. Electrochem. Sci.*, 10 **(2015)** 969 - 981

International Journal of
ELECTROCHEMICAL
SCIENCE
www.electrochemsci.org

# Using a Cosolvent that Contains Ionic Liquid and Distilled Water as the Media to Prepare Multi-walled Carbon Nanotubes Supported Pd Nanoparticles by a Hydrothermal Process for Ethanol Oxidation Reaction (EOR)

*Keqiang Ding*[1,*], *Yongbo zhao*[1], *Yuan Li*[1], *Jing Zhao*[1], *Yuying Chen*[1], *Yiran Wang*[3], *Zhanhu Guo* [2, 3,*]

[1]College of Chemistry and Materials Science, Hebei Normal University, Shijiazhuang 050024, P.R. China
[2] Integrated Composites Laboratory (ICL), Department of Chemical and Biomolecular Engineering, University of Tennessee Knoxville, Knoxville, NT 37996 USA.
[3] Integrated Composites Laboratory (ICL), Dan F. Smith Department of Chemical Engineering, Lamar University, Beaumont, TX 77710, USA
[*]E-mail: dkeqiang@263.net; zhanhu.guo@lamar.edu

*Received:* 5 October 2014 / *Accepted:* 17 November 2014 / *Published:* 2 December 2014

For the first time, multi-walled carbon nanotubes supported palladium nanoparticles (denoted as Pd/MWCNTs) were prepared by a hydrothermal process, in which a mixed solution containing a kind of ionic liquid and distilled water was used as the solvent. It should be mentioned that except MWCNTs no other reducing agents were involved in the preparation process. The crystal structure, morphology and particle sizes of the as-prepared samples were featured by X-ray diffraction (XRD) and transmission electron microscope (TEM). The electrocatalytic activities of Pd/MWCNTs catalysts towards EOR were investigated in an alkaline medium using cyclic voltammetry (CV) and chronoamperometry (CA). The results demonstrated that the catalyst prepared by the hydrothermal process for 3 h showed the best electrocatalytic activity towards EOR among the as-prepared catalysts.

**Keywords:** Hydrothermal method; nanoparticles; electro-catalyst; cosolvent; ionic liquid; ethanol oxidation reaction.

## 1. INTRODUCTION

It is well known that water and organic solution like acetone are the main two kinds of solvents that have been widely used in the traditional chemical system. Recently, room temperature ionic

liquids (RTILs), as a novel media different from water and organic solvent, have been intensively applied in many research systems due to their excellent features such as low-volatility, non-toxicity, inflammability, higher conductivity compared to common organic solvents, and higher solubility for organic substances when compared with aqueous solutions [1]. Summarily, being used as the solvent in organic synthesis [2] and being employed as an electrolyte in electrochemistry [3] are the major two contributions of RTILs when used in the research field of chemistry. For example, Li et al. [4] developed an ionic liquid-supported synthetic method for the construction of glycopeptides. Singh and his coworkers [5] presented a practical and novel approach for the synthesis of vinyl sulfides by the reaction of sulfonyl hydrazides with aryl/heteroarylacetylenes using a DBU-based ionic liquid. Swiderska-Mocek et al. [6] prepared a binder-free activated carbon cloth-sulphur (ACC-S) composite cathode, and studied the electrochemical properties of ACC-S in an ionic liquid electrolyte consisting of 1-ethyl-3-methylimidazolium bis(trifluoromethanesulphonyl)imide ($EtMeImNTf_2$) and bis(trifluoromethanesulphonyl)imide ($LiNTf_2$). Nohira and his coworkers [7] synthesized $Na_2MnSiO_4$ by a sol-gel method and investigated its electrochemical performance as a positive electrode material for Na secondary batteries using Na[FSA]–[$C_3C_1$pyrr][FSA] ionic liquid electrolyte in the temperature range 298-363 K. To the best of our knowledge, in the synthesis field of Pd nanoparticles, the cosolvent that contains RTILs and water is rarely explored

As a power source for mobile and portable electronic applications, fuel cells, based on the electrooxidation of small organic molecules such as methanol, ethanol and formic acid, has received increased attention nowadays [8]. Ethanol-based fuel cells, namely, direct ethanol fuel cells (DEFCs), has been demonstrated to have many unique advantages such as the low toxicity, high energy density, biocompatibility and abundant availability [9]. More importantly, ethanol can be produced in large quantities from the fermentation of biomass and all related substances like ethanol and carbon dioxide( final product) are relatively non-toxic. Therefore, developing anode catalysts for ethanol oxidation reaction (EOR) is very crucial to the further commercialization of DEFCs. Although platinum (Pt) has been recognized as the most active catalyst for ethanol oxidation, the high cost and limited supply of Pt have substantially hindered the development of DEFCs [9]. Fortunately, palladium (Pd) is indicated to present a higher electrocatalytic activity and better stability for ethanol electro-oxidation in alkaline media, which made Pd a promising alternative to Pt anode catalyst especially since the commercialization of alkaline anion exchange membranes (AAEMs) [10]. Also, Pd is much more abundant on the earth which can greatly reduce the producing cost of anode catalysts. Therefore, developing novel methods for preparing Pd nanoparticle catalysts has turned into a hot topic in the research field of electrocatalysis. Till now, there are two main methods, viz. chemical reduction method and the electrochemical reduction method, for preparing Pd nanoparticles. For example, Marinšk's group [11] prepared several CNT-supported Pd-based catalysts via various impregnation methods, in which a reducing agent of hydroquinone was mainly used. Feng et al. [12] reported that Pd catalysts could be procured after 20 cycles of cyclic voltammetry (CV) in a potential range at the scan rate of 50 $mVs^{-1}$, in which the eletrodeposition solution contained 0.5 M $H_2SO_4$ and 5mM $K_2PdCl_4$. Some other methods such as the microemulsion method [13], the colloidal method [14], ionexchange [15] and thermal decomposition [16] were also developed for synthesizing supported Pd catalysts.

Although many novel kinds of carbon such as carbon nanofiber [17] and graphene [18] have been created recently, carbon nanotubes (CNTs) [19] still attracted tremendous interest due to their unique properties, such as high external surfaces, good electronic conductivity, and high stability. Summarily, being utilized as a supporting material is the main contribution of CNTs when used in the field of electrochemistry [20].

In the present work, the Pd/MWCNTs nanoparticles catalysts were successfully fabricated by a facile method of hydrothermal reaction in the presence of MWCNTs, in which a cosolvent that contained distilled water and ionic liquid was employed. It should be underlined that the preparation system only consisted of distilled water, ionic liquid, MWCNTs and palladium salt of $PdCl_2$. And no other reducing agents were introduced in above system. XRD and TEM measurements were, respectively, utilized to characterize the crystalline structures and morphologies of the resultant samples. The electrocatalytic activities of the as-prepared Pd/MWCNTs catalysts towards EOR in 1M KOH were investigated by using cyclic voltammetry (CV) and chronoamperometry (CA), and the results indicated that the Pd/MWCNTs catalysts that were prepared by the hydrothermal process for 3h exhibited the highest electrocatalytic activity among all the samples.

## 2. EXPERIMENTAL SECTION

### *2.1 Materials*

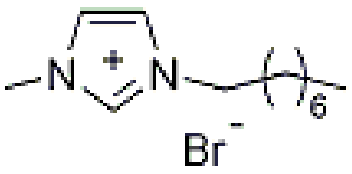


**Scheme 1.** Molecular structure of ionic liquid [OMIM]Br

Room temperature ionic liquid of 1-Octyl-3-methylimidazolium Bromide (denoted as [OMIM]Br, as shown in scheme 1.) with a purity of more than 99% was purchased from Shanghai Cheng Jie Chemical Co. LTD (China). MWCNTs (purity>95%) with an average diameter of 10-20 nm were bought from Shenzhen nanotech port Co., Ltd (China). All the electrodes were purchased from Tianjin Aida Co., Ltd (China). All the chemicals were of analytical grade and used as-received without any further treatment. Doubly-distilled water was used to prepare the aqueous solutions.

### *2.2 Preparation of Pd/MWCNTs nanoparticles*

Firstly, 6.0mg of $PdCl_2$ and 15 mg MWCNTs were dissolved in a cosolvent that consisted of 3mL [OMIM]Br and 1mL distilled water, and then the resulting mixture was ultrasonicated for 30 min, generating a suspension solution. Secondly, the resultant suspension solution was transferred into a home-made autoclave at room temperature, and subsequently the well-sealed autoclave was placed in a muffle furnace. Lastly, the temperature of the muffle furnace was maintained at 200 ºC for various

periods to accomplish the hydrothermal process, which was implemented in an SRJX-8-13 furnace equipped with a KSY 12-16 furnace temperature controller. After cooling down to the room temperature, the filtered samples were thoroughly washed with distilled water, and dried in an ambient condition to generate the MWCNTs supported Pd catalysts (denoted as Pd/MWCNTs). The catalysts prepared by the hydrothermal reaction for 1, 2, 3 and 4h were denoted as sample **a**, **b**, **c** and **d**, respectively.

### *2.3 Preparation of Pd/ MWCNTs modified electrode*

Prior to each experiment, a glassy carbon (GC) electrode (geometric area of 0.07 $cm^2$) was thoroughly burnished using 50 nm alumina nanopowder suspensions and then served as a substrate for the working electrode. The working electrodes were prepared by casting the catalyst ink onto a GC electrode. The catalyst ink was obtained by dispersing 1 mg catalyst in 1 mL Nafion ethanol solution (0.1 wt.%). And after ultrasonication for 10 min, about 15 μL catalyst ink was dropped onto the surface of a GC electrode and slowly dried in air, yielding a Pd/MWCNTs-coated GC electrode.

### *2.4 Characterizations*

XRD analysis of the catalyst was carried out on a Bruker D8 ADVANCE X-ray diffractometer equipped with a Cu Kα source (λ= 0.154 nm) at 40 kV and 30 mA. The 2$\theta$ angular region between 10 and 90° was explored at a scan rate of 1°/step. The particle morphology was observed by transmission electron microscopy (TEM, HITACHI, H-7650). UV–vis spectra were obtained on a spectrophotometer V-500 (JASCO, Japan)

Electrochemical measurements were all carried out on a CHI 660B electrochemical workstation (Shanghai Chenhua Apparatus, China) connected to a personal computer. EIS was performed in the frequency range from 0.05 to $10^5$ Hz with an amplitude of 10 mV.

A traditional three-electrode system was employed, in which a Pd/MWCNTs modified GC electrode and a platinum wire were used as the working electrode and counter electrode, respectively. The reference electrode was a saturated calomel electrode (SCE). All potentials in this paper were reported with respect to SCE. A solution of 1 M KOH containing 1 M ethanol was used to study ethanol oxidation activity.

## 3. RESULTS AND DISCUSSION

### *3.1 XRD Analysis*

Fig.1 presents the XRD patterns of the samples involved. Pattern **o** corresponds to the pure MWCNTs, in which a diffraction peak located at around 26° is displayed clearly. According to our previous work, this diffraction peak is assigned to the (002) facet of MWCNTs [21]. Evidently, after the hydrothermal process, four diffraction peaks are observed in each XRD pattern, indicating the formation of new substances.

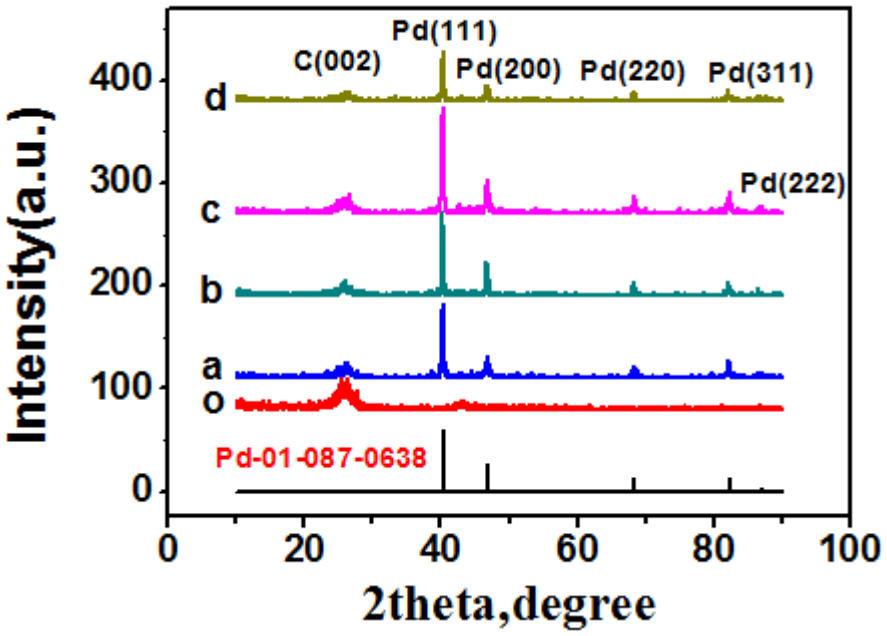


**Figure 1.** XRD patterns of the pure MWCNTs (pattern **o**) and the obtained samples. Patterns **a**, **b**, **c** and **d** correspond to the catalysts of Pd/MWCNTs prepared by the hydrothermal process for **1**, **2**, **3** and **4** h.

The four diffraction peaks centered at $2\theta$ values of about 40.3°, 46.8°, 68.4° and 82.5°, respectively, exactly corresponded to the planes (111), (200), (220) and (311) of the face centered cubic (fcc) crystalline Pd (JCPDS, Card No.01-087-0638), being consistent with the former report [22] very well. This result effectively demonstrated that the developed method of hydrothermal process was a feasible way to prepare metallic palladium. Meanwhile, besides the characteristic diffraction peaks of fcc Pd, no diffraction peaks corresponding to the Pd oxides or Pd hydroxides were displayed, suggesting that the amount of Pd oxides or Pd hydroxides was too small to be detected, or their existence in amorphous phases[23]. Compared to the aqueous solutions, ionic liquids have less content of dissolved oxygen [24], which may be responsible for above result that no Pd oxides or Pd hydroxides were detected by using XRD measurement. Close inspection revealed that the intensities of the diffraction peaks for the as-prepared samples were different from each other. This result strongly indicated that the period of hydrothermal process played a key role in determining the crystal structure of the resultant samples. It is clear that the intensities of all the diffraction peaks for the sample **c**, such as the peak at around 40.3°, are obviously higher than that of other samples. Also, a diffraction peak corresponding to the plane (222) of the face centered cubic (fcc) crystalline Pd is evidently displayed in the case of sample **c**. All these results remarkably indicated that the crystallinity of sample **c** is the best among all the four catalysts [25].

The average particle sizes of the catalysts were calculated from the facet Pd (111) peak by the Scherrer formula [26]:

$$d(\mathring{\mathrm{A}}) = \frac{\kappa\lambda}{\beta\cos\theta}$$

where $\kappa$ is a coefficient (0.9), $\lambda$ the wavelength of X-ray used (1.54056 Å), $\beta$ the full-width half maximum and $\theta$ is the angle at position of peak maximum. The calculated particle sizes based on the plane of (111) for sample **a**, **b**, **c** and **d** were 30.4, 30.3, 25.5 and 40.6 nm, respectively. Therefore, the particle size of sample **c** prepared by the hydrothermal process for 3 h is the smallest among all the prepared samples. It indicated that sample **c** may provide a larger surface area relative to other catalysts at the same particle loadings.

*3.2 TEM Analysis*

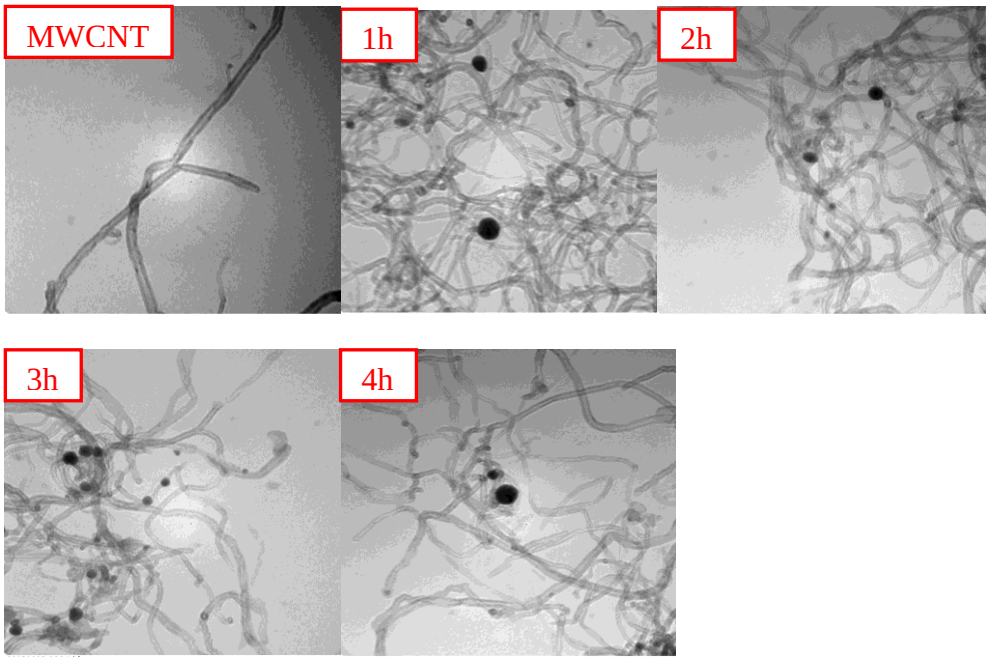


**Figure 2.** TEM images of the pure MWCNTs and the obtained samples. The direct magnification was 200000x.

Fig.2 shows the TEM images of the samples appearing in this experiment. It is evident that no particle was anchored on the surface of pure MWCNTs. After the hydrothermal process, some black spherical particles are observed to be immobilized on the surface of MWCNTs when compared to the pure MWCNTs. It effectively proved that some substances were fabricated using this facile method of hydrothermal reaction. Based on the TEM images, the particle sizes for the catalysts of sample **a**, **b**, **c** and **d** are estimated to be about 28, 21, 16 and 35nm, respectively. Thus, the sample **c** has the smallest size among the prepared samples, which was consistent with the result calculated from the XRD patterns. The fact that the mean particle sizes estimated from TEM images were smaller than that calculated from XRD pattern could be attributed to the fact that XRD reflects crystalline particles, not the actual morphology of catalysts. And in the XRD measurement large particles are selected, while most of the small particles are counted in TEM images [27].

*3.3 Electrocatalytic performance of Pd/MWCNTs catalysts towards EOR*

To study the electrochemical process of EOR on the prepared catalysts, the cyclic voltammograms (CVs) obtained on the sample **c** modified GC electrode are illustrated in Fig. 3.

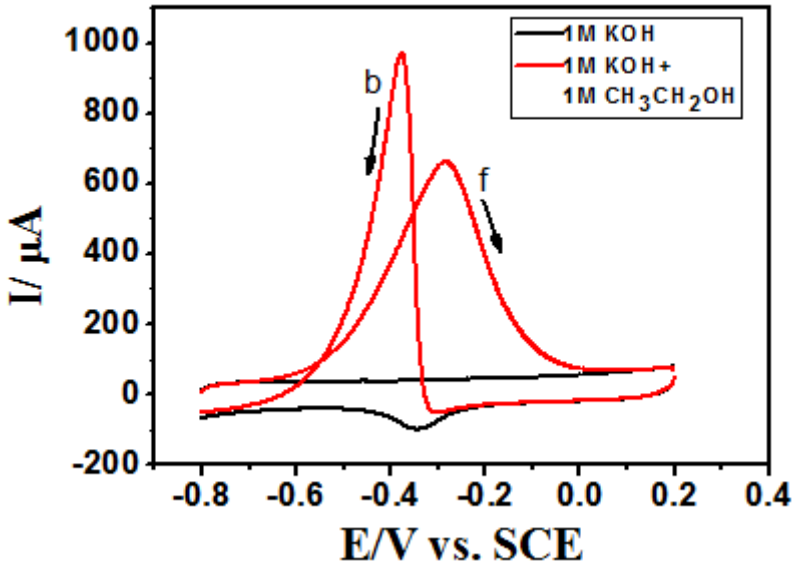


**Figure 3.** CVs obtained on the 3h-prepared Pd/MWCNTs coated GC electrode in the solution of 1M KOH ( black curve ) and 1M KOH +1M $C_2H_5OH$ (red curve) at the scan rate of 100 $mVs^{-1}$.

It is evident that no oxidation peaks were found in 1 M KOH solution, and only a cathodic peak corresponding to the electro-reduction of PdO was exhibited [23]. In the presence of ethanol, two well-defined oxidation peaks, one oxidation peak (peak **f**) centered at ~-0.289 V in the anodic potential sweep and one oxidation peak (peak **b)** located at ~ -0.378 V in the cathodic potential sweep, are clearly observed, strongly demonstrating that EOR can occur on the prepared catalyst of Pd/MWCNTs. The shape of CVs for EOR on the prepared catalysts accorded with the previous report very well [28]. It strongly indicated that the resulting catalyst has the electrocatalytic ability toward EOR.

Fig.4 presents the CV curves of EOR obtained on all the prepared catalysts, in which the oxidation peaks for EOR are clearly exhibited. This result substantially indicated that all the prepared samples had electrocatalytic activity toward EOR. However, careful analysis indicated that the catalysts prepared by the hydrothermal process for different periods have various electrocatalysis activities towards EOR. In general, the forward oxidation current peak **f** is assigned to the oxidation of freshly chemisorbed species coming from ethanol adsorption, and the reverse oxidation peak **b** is primarily associated with the removal of carbonaceous species not completely oxidized in the forward scan, rather caused by freshly chemisorbed species [29]. Obviously, the sample **c** displayed the largest peak currents among all the prepared samples, implying that 3h-prepared Pd/MWCNTs catalyst has the highest electrocatalytic ability toward EOR as compared to other catalysts. Besides the peak current, the onset potential of the first oxidation peak in the anodic sweep is another key parameter that can reflect the catalytic activity of a catalyst towards EOR [30]. Also, the 3h-prepared catalyst, i.e.,

sample **c**, showed the most negative onset potential of EOR, suggesting that EOR may proceed more easily on sample **c** as compared to that on other catalysts. Also, it was reported that the incomplete oxidized carbonaceous species, such as $CH_3CO_{ads}$, could accumulate on the electrode and poison the electrode. And the ratio of the forward anodic peak current (peak **f**) to the reverse anodic peak current (peak **b**), i.e., $I_f/I_b$, could be used to evaluate the poisoning tolerance of catalyst [31]. A larger $I_f/I_b$ ratio indicates a better oxidation ability of ethanol during the anodic scan. The ratios of peak **f** to peak **b** for sample **a**, **b**, **c** and **d** were estimated to be about 0.678, 0.766, 0.676 and 0.714, respectively. It seemed that sample **b** should present the best electrochemical performance. In contrast, sample **c** delivered the best electrocatalytic activity for EOR, as was testified by the largest polarization current in the galvanostatic measurement (Fig. 4.). This result also indicated that the previous proposition that employs the ratio of $I_f/I_b$ to value the electrochemical activity of a catalyst towards EOR is not comprehensive.

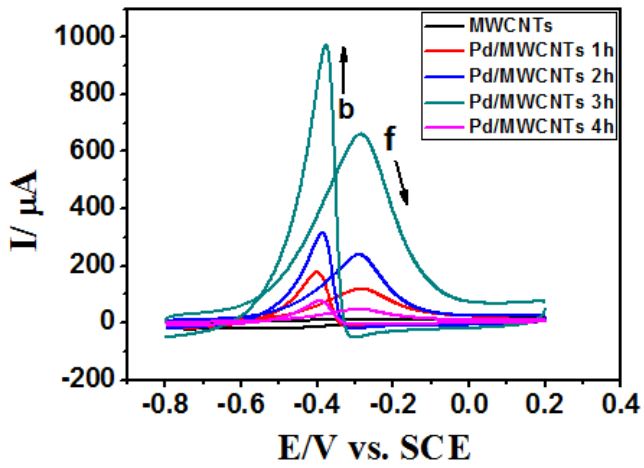


**Figure 4.** CVs obtained on the pure MWCNTs, various Pd/MWCNTs catalysts coated GC electrode in the solution of 1M KOH +1M $C_2H_5OH$ at the scan rate of 100 $mVs^{-1}$.

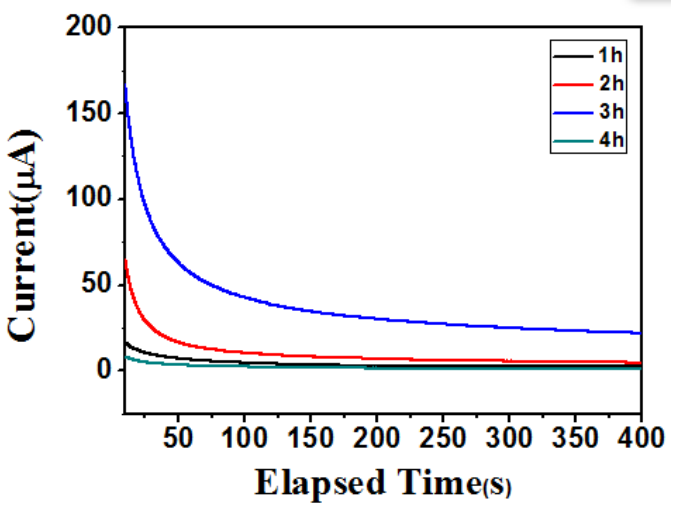


**Figure 5.** Chronoamperometry curves of as-prepared samples-coated GC electrode in 1M KOH +1M $C_2H_5OH$ at the potential of -0.28V vs. SCE.

Chronoamperometric (CA) measurement is a typical method that can be used to probe the tolerance of a catalyst in the electrooxidation process of small organic molecules [32]. Fig.5 shows the current decay at a fixed potential of -0.28V of GC electrodes modified with as-prepared catalysts in 1M KOH containing 1M ethanol. It is evident that the polarization currents at all the catalysts decayed rapidly during the initial period (within 50s). Generally, the decrease in current at the initial stage is closely related to the charging/discharging process of the double-layer existing at the interface between the electrode and electrolyte. It was also stated that the decrease in current is mainly due to the surface poisoning induced by the intermediate CO species, and the lower current decay rate of a catalyst may be owing to the effective cleaning of the electrode surface. Meanwhile, according to the electrochemical theory, the currents obtained from electrochemical measurements were all originated from the electrochemical oxidation /reduction of active materials. Thus, under the same conditions, the current value is proportional to the amount of active materials participating in the electrochemical reaction. Thus, the higher current at the beginning of the CA test should correspond to a higher concentration of active materials adsorbed at the surface of the catalyst coated electrode. Therefore, more amounts of substances including ethanol and the intermediates such as CO were anchored on the surface of sample **c**, which led to a higher polarization current at the initial stage. The relatively stable polarization current presented after the initial stage should be mainly attributed to the electrooxidation of ethanol molecules that have diffused from the bulk solution to the electrode. Clearly, during the whole testing period, the polarization current for EOR on the electrocatalyst of sample **c** remained much higher than that of other catalysts. This result probably was due to the smaller particle size (Fig.2) and higher crystallinity (Fig.1) of sample **c** as compared to other catalysts.

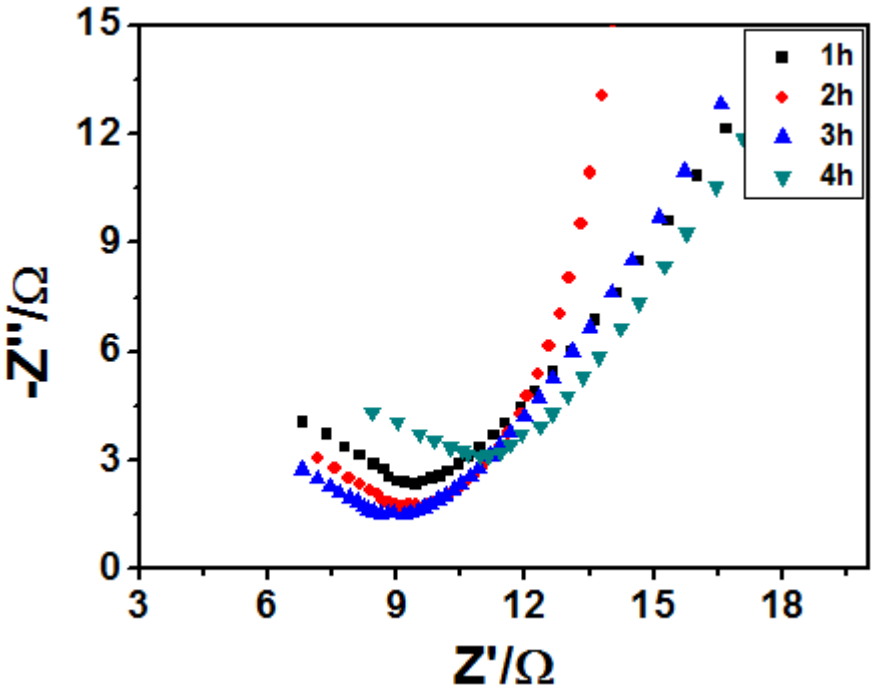


**Figure 6.** Nyquist plots obtained on the various catalysts modified GC electrodes in the solution of 1M KOH containing 1M ethanol at the open circuit potentials.

Fig.6 gives the Nyquist plots of the EOR on all the prepared catalysts modified GC electrodes. As shown in Fig. 6, it is clear that for all the electrodes, the Nyquist plots were constructed by a semicircle and a nearly 45º line, which is the typical shape of Nyquist plot for an electrochemical reaction that take places at the interface between electrolyte and electrode [33]. Generally, the semicircle appearing at the high frequency region should represent a circuit consisting of a resistance element parallel to a capacitance element, and the larger diameter of the semicircle should correspond to a larger charge transfer resistance ($R_{ct}$)[33]. The sloped line in the lower frequency region was originated from the Warburg resistance, which is closely related to the diffusion process of molecules in the electrochemical reaction. Evidently, the values of the diameter for the semicircles were different from each other. Approximately, the values of diameters for sample **a**, **b**, **c** and **d** were estimated to be 6.38 Ω, 4.70 Ω, 4.35 Ω and 7.40 Ω, respectively. Consequently, the value of charge transfer resistance ($R_{ct}$) for EOR on the 3h-prepared catalyst was the lowest one among all the prepared catalysts. It effectively indicated that the electron transfer process of EOR on the sample **c** modified GC electrode became easier when compared to that on other catalysts. According to the values of $R_{ct}$, it can be deduced that the electrocatalytic activity of the prepared catalysts towards EOR was in the decreasing order of sample **c** (3h) > **b** (2h) > **a** (1h) > **d** (4h). This electrocatalytic activity order is almost consistent with that order deduced from CA test (Fig.5). In other words, the electrocatalytic activities of the catalysts prepared in this work for EOR were closely related to the hydrothermal reaction time since the hydrothermal reaction period could greatly influence the particle size, crystallinity and morphologies of the resulting nanoparticle catalysts.

*3.4 Analysis of Pd/MWCNTs formation process*

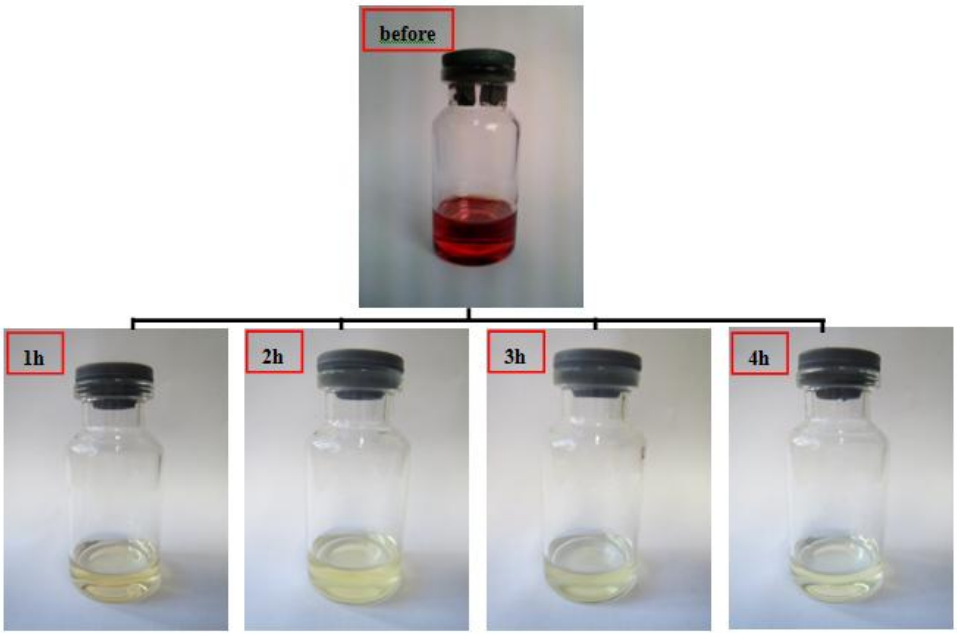


**Figure 7.** Photographs of the filtered solutions used in this experiment (before and after the hydrothermal reaction).

How does one understand the formation process of the as-prepared nanoparticles in this simple process of hydrothermal reaction? Fig. 7 presented the photos of the filtered solutions before and after the hydrothermal process. It can be seen that a carmine transparent solution was produced after $PdCl_2$ was dissolved in the cosolvent having ionic liquids and distilled water. Interestingly, after the hydrothermal process, a bright-yellow solution was presented, implying that most metal ions of Pd were reduced. Interestingly, a nearly transparent solution was exhibited when the hydrothermal period was up to 4 h. Fig.8 shows the corresponding ultraviolet-visible (UV-vis) absorption spectra of the solution before and after hydrothermal process. Clearly, for the starting solution, one absorption peak located at around 218 nm was observed. Commonly, the spectra in the far-UV region (200-250 nm) corresponds to the peptide n→π* electronic transition[34], probably the empty orbit of the $Pd^{2+}$ have reacted with the lone pair electrons of the nitrogen atoms in [OMIM]Br molecule. While, for the sample treated by hydrothermal process for 1 h, the intensity of the peak was decreased significantly, suggesting that most ions of $Pd^{2+}$ disappeared in this process, though a small peak positioned at about 203 nm was still displayed. Obviously, no absorption peak was observed when the hydrothermal reaction time was above 2h. Obviously, the absorbance intensity of the absorption peak decreased significantly with the increasing of hydrothermal reaction period. This result was in accordance with that observed from the photos in Fig.7.

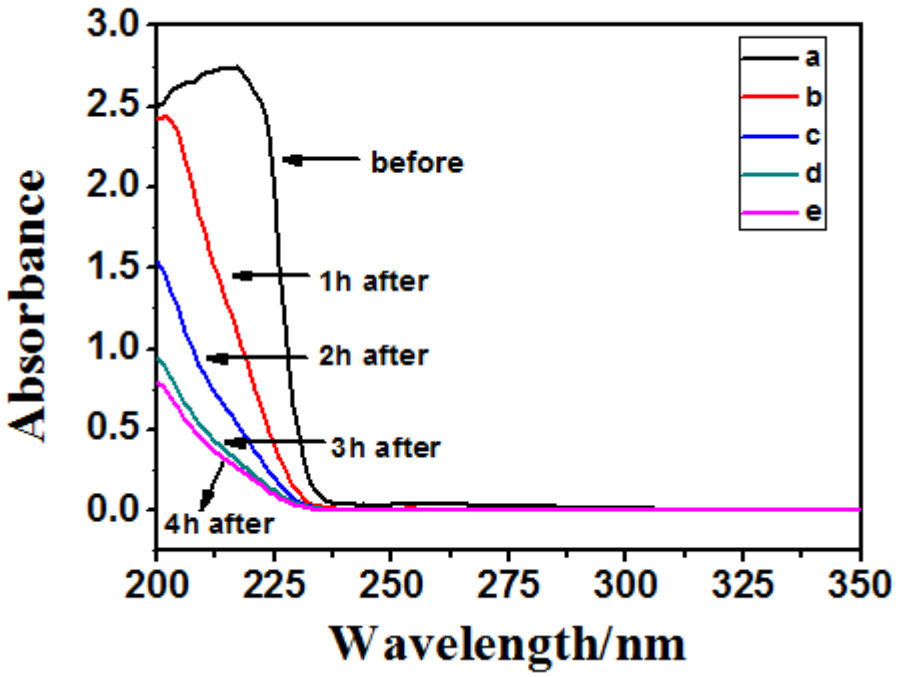


**Figure 8.** UV-vis spectra for the filtered solutions after various periods of hydrothermal process.

According to the previous report, in the presence of MWCNTs, a reductive environment could be produced by some reactions between the cosolvent and carbon such as $C+H_2O=CO+H_2$ [35]. Thus, the produced CO and $H_2$ may reduce the $Pd^{2+}$ ions in the hydrothermal process, leading to the formation of Pd nanoparticles. Therefore, it was reasonable to believe that under proper conditions Pd

nanoparticles could be fabricated by this simple hydrothermal process, which is probably very beneficial to the industrial production of nanoparticles due to its simplicity in manufacture.

## 4. CONCLUSION

For the first time, a cosolvent that contained ionic liquid and distilled water was utilized as a new media for preparing Pd nanoparticles by a facile method of hydrothermal reaction in the presence of MWCNTs. In this work, the influences of hydrothermal reaction period on the morphologies and the electrocatalytic activities of the resulting samples were thoroughly investigated. Characterization analysis revealed that the catalyst prepared by the hydrothermal reaction for 3h had the smallest particle size and best crystallinity among all the prepared nanoparticle catalysts. Results obtained form CV and CA indicated that 3h-prepared catalyst had better electrocatalytic activity toward EOR than other catalysts. Comparison of the photos before and after the hydrothermal reaction impressively confirmed that $Pd^{2+}$ ions were totally reduced in the hydrothermal process. Opening a new path for the synthesis of promising electrocatalysts for fuel cells is the main contribution of the present work.

ACKNOWLEDGMENTS
This work was financially supported by the National Natural Science Foundation of China (No. 21173066), Natural Science Foundation of Hebei Province of China (No.B2011205014). Z. Guo acknowledges the support from US National Science Foundation (EAGER:CBET 11-37441) managed by Dr Rosemarie D. Wesson.

## References

1. B. Xin and J. Hao, *Chem. Soc. Rev.*, 43(2014)7171.
2. M. Carmen Galan, R. A. Jones and A.-T. Tran, *Carbohydr. Res.*, 375 (2013) 35.
3. A. Basile, A. F. Hollenkamp, A. I. Bhatt and A. P. O'Mullane, *Electrochem. Commun.*, 27 (2013)69.
4. C. Li , Z. Zhang, Q. Duan and X. Li , *Org. Let.*, 16 (2014)3008.
5. R. Singh , D. S. Raghuvanshi and K. N. Singh, *Org. Let.*, 15 (2013) 4202.
6. A. Swiderska-Mocek and E. Rudnicka, *J. Power Sources*, 273 (2015) 162.
7. C.-Y. Chen, K. Matsumoto, T. Nohira and R. Hagiwara, *Electrochem. Commun.*, 45 (2014) 63.
8. Y.-J. Wang, J. Qiao, R. Baker and J. Zhang, *Chem. Soc. Rev.*, 42(2013)5768.
9. W. Du, G. Yang, E. Wong , N. Aaron Deskins, A. I. Frenkel . D. Su and X. Teng, *J. Am. Chem. Soc.*, 136(2014)10862.
10. R.Carrera-Cerritos, R.Fuentes-Ramírez, F.M.Cuevas-Muñiz, J.Ledesma-García and L.G. Arriaga, *J. Power Sources*, 269 (2014) 370.
11. M. Marinšk, M. Šala and B. Jančar, *J. Power Sources*, 235 (2013) 111.
12. Y.-Y. Feng, Q.-Y. Yin, G.-P. Lu, H.-F. Yang, X. Zhu, D.-S. Kong and J.-M. You, *J. Power Sources*, 272 (2014) 606.
13. Y. Liu, X. Qiu, Z. Chen and W. Zhu, *Electrochem. Commun.*, 4 (2002) 550.
14. Y. Huang, X. Zhou, J. Liao, C. Liu, T. Lu and W. Xing, *Electrochem. Commun.*, 10 (2008) 621.
15. A. Sartre, M. Phaner, L. Porte and G.N. Sauvion, *Appl. Surf. Sci.*, 70-71(1993) 402.

16. B. Xue, P. Chen, Q. Hong, J. Lin and K. L. Tan, *J. Mater. Chem.*, 11 (2001) 2378.
17. G.-H. An and H.-Jin Ahn, *J. Power Sources*, 272 (2014) 828.
18. W. Guo, H. Li, M. Li, W. Dai, Z. Shao, X. Wu and B. Yang, *Carbon*, 79(2014)636.
19. K. Harano, S. Takenaga, S. Okada, Y. Niimi, N. Yoshikai, H. Isobe, K. Suenaga, H. Kataura, M. Koshino and E. Nakamura, *J. Am. Chem. Soc.*, 136(2014) 466.
20. J. Zhang, S. Tang, L. Liao,W. Yu, J. Li, F. Seland and G. M. Haarberg, *J. Power Sources*, 267 (2014) 706.
21. K. Ding, M. Cao, *Russ. J. Electrochem.*, 44 (2008) 977.
22. S.-S. Li, J. Yu, Y.-Y. Hu, A.-J. Wang, J.-R. Chen and J.-J. Feng, *J. Power Sources*, 254 (2014) 119.
23. Z. Zhang, L. Xin, K. Sun and W. Li，*Int. J. Hydrogen Energy* , 36 (2011) 12686.
24. K. Ding, T. Okajima and T. Ohsaka, *Electrochemistry*, 75 (2007) 35.
25. K. Tang, J. Sun, X.Yu, H. Li, X. Huang, *Electrochim. Acta*, 54 (2009) 6565.
26. Y. Zhao, L. Zhan, J. Tian, S. Nie and Z. Ning, *Electrochim. Acta*, 56 (2011) 1967.
27. J. Tayal, B. Rawat and S. Basu, *Int. J. Hydrogen Energy*, 36 (2011) 14884.
28. W. Hong, Y. Fang, J. Wang and E. Wang, *J. Power Sources*, 248 (2014) 553.
29. R.N. Singh and A. Singh, *Int. J. Hydrogen Energy*, 34 (2009) 2052.
30. M. Nie, H. Tang, Z. Wei, S. P. Jiang and P. K. Shen, *Electrochem. Commun.*, 9 (2007) 2375.
31. G-Y. Zhao, C-L. Xu, D-J. Guo, H. Li and H- L. Li, *J. Power Sources*, 162 (2006) 492.
32. K. Ding, G. Yang, S. Wei, P. Mavinakuli and Z. Guo，*Ind. Eng. Chem. Res.*, 49 (2010) 11415.
33. K. Ding, Z. Jia, Q.Wang, X. He, N. Tian, R. Tong and X. Wang，*J. Electroanal. Chem.*, 513 (2001) 67.
34. X. Wu, P. Du, P. Wu and C. Cai, *Electrochim. Acta*, 54 (2008) 738.
35. Z. Zhu, G.Q. Lu, J. Finnerty and R. T. Yang, *Carbon*, 41 (2003) 635.